Keck High Resolution Spectroscopy of PKS 0123+257: Intrinsic Absorption in a Radio Loud Quasar

Thomas A. Barlow[1] and W. L. W. Sargent[1]
Astronomy Department, California Institute of Technology, Pasadena, CA 91125

ABSTRACT

We present results from Keck I high resolution spectroscopy of the radio loud quasar PKS 0123+257 (z_e=2.364, V=17.5). In this object we detect Lyα, N v $\lambda\lambda$1238,1242, Si iv $\lambda\lambda$1393,1402, and C iv $\lambda\lambda$1548,1550 in an absorption system at a redshift of 2.369. The Lyα line has a square-bottomed profile suggesting a high column density of gas, yet the line does not reach zero intensity. The resolved C iv doublet ratio also clearly demonstrates that the absorbing clouds at this redshift do not fully occult the background light source along our line-of-sight.

The absorption lines are positioned near the centers of the broad emission-lines and the coverage fraction of the strongest absorption lines varies inversely proportionally with the strength of the corresponding emission lines. This implies that although the absorption-line region may obscure the continuum source, it does not completely occult the broad emission-line region. This effect suggests that the lines are formed close to the QSO central region. A model is proposed in which the *apparent* coverage fraction derived for the weaker absorption lines may vary with the column density of the lines.

Broad absorption-lines (which are known to be intrinsic) are found nearly exclusively in radio-quiet objects. Intrinsic narrow absorption lines have previously been found in radio quiet QSOs; it is therefore significant that an intrinsic absorption system has been verified in a radio loud quasar.

Subject headings: quasars: absorption lines — quasars: individual (PKS 0123+257)

Accepted to the Astronomical Journal (January 1997 issue.)

[1]Visiting Astronomer, W.M.Keck Observatory, jointly operated by the California Institute of Technology and the University of California

1. Introduction

PKS 0123+257 (V=17.5, $z_e = 2.364$), or 4C 25.05, is a radio loud quasar (Schmidt and Olsen 1968; Carswell et al. 1976.) This object shows a strong, narrow absorption-line system with an absorption-line redshift (z_a) close to the emission-line redshift (z_e.) We selected this object for study with the High Resolution Echelle Spectrograph (HIRES) on the Keck I telescope in an effort to investigate the nature of intrinsic absorption systems.

We define an "intrinsic" absorption system as one which is caused by clouds in the QSO environment, either near the continuum source or elsewhere in the host galaxy. This is to be distinguished from systems which arise from intervening galaxies and intergalactic clouds. Intrinsic systems can either be very broad (∼10,000 km s^{-1}) as in the so called "broad absorption-line" (BAL) QSOs, or they can be relatively narrow (∼ 100 km s^{-1}) with a number of cases being intermediate in width.

Intrinsic absorption systems can be used to study the QSO environment, test standard models of quasars, and estimate metallicities in quasar environments. Recent work has strongly suggested that gas near a QSO has heavy element abundances much enhanced relative to the solar value (Petitjean et al. 1994; Hamann 1996 and references therein.) Intrinsic narrow lines are potentially more useful in metallicity estimates than BALs since it is often possible to separate the components of close doublets such as C IV $\lambda\lambda$1548,1550 and N V $\lambda\lambda$1238,1242. In practice it can be ambiguous as to whether a particular narrow line absorption system with $z_a \sim z_e$ is intrinsic or intervening. For these reasons, it is important to develop means of distinguishing the two categories.

The best candidates for intrinsic narrow lines are systems with $z_a \sim z_e$. This category of "associated" absorption has been defined as lines which appear within several thousand km s^{-1} of the emission redshift and are less than a few hundred km s^{-1} wide (cf. Foltz et al. 1988; Anderson et al. 1987.) Since we expect some intervening lines to appear close to the emission redshift, these "associated" lines may not always be intrinsic to the QSO. Occasionally we observe strong, complex absorption, commonly with high excitation, which are thought to be intrinsic because such systems are rarely seen at $z_a \ll z_e$ (*e.g.* PKS 1157+014, cf. Briggs et al. 1984 and GC 1556+335, cf. Morris et al. 1986.) Previous work on narrow associated absorption has attempted to establish the intrinsic nature of the lines statistically. There appears to be an excess of narrow lines near z_e in large samples of QSOs (Weymann et al. 1979; Foltz et al. 1986.) Although this result has been questioned by other surveys (Sargent et al. 1988), it is now apparent that systems with large total equivalent width tend to be close to the emission redshift (cf. Foltz et al. 1988; Barthel 1988). Furthermore, there appears to be an excess of associated lines in radio-loud quasars (Anderson et al. 1987) relative to radio-quiet QSOs; such an excess could only be explained by an intrinsic origin.

The following ways have been proposed to distinguish intrinsic from intervening absorption systems (in order of decreasing reliability): (1) time variability (Hamann et al. 1995; Hamann et al. 1996b), (2) high electron density as derived from fine structure lines as a distance indicator when combined with an ionization level estimate (cf. Bahcall 1968; Williams et al. 1975; Morris et al. 1986), (3) partial coverage of the background light source along our line-of-sight by the absorption-line region (cf. Wampler et al. 1993; Wampler et al. 1995; Hamann et al. 1996; Hamann et al. 1996b), (4) spectropolarimetry revealing increased fractional polarization in the lines relative to the continuum (so far only observed in BALs, cf. Goodrich and Miller 1995, Cohen et al. 1995), (5) velocity structure, *i.e.* breadth, complexity, and "correlated" or "smooth" profile shape across many components, (6) higher ionization level, and (7) higher metallicities (*e.g.* Petitjean et al. 1994.)

Although time variability has been observed often in BALQSOs (Barlow et al. 1992; Barlow 1993), method (1) generally requires extensive monitoring of a large sample of objects over at least a few years. Method (2) requires the presence of fine structure lines (usually) of C II or Si II. Unfortunately, the high ionization and/or low column density of many systems makes these lines difficult to detect. Method (4) requires long exposure times with low resolution and can only be used on objects with relatively high polarization and, therefore, has only been useful for studying a few wide BALs. Method (6) and (7) are easy to apply but are very sensitive to photoionization models (*e.g.* Hamann 1996) and there may be a large overlap in these qualities between intrinsic and intervening systems. Fortunately, methods (3) and (5) can be applied directly and easily using Keck and HIRES. Recently it has become evident that high resolution

spectra with high signal-to-noise ratios can be a useful tool in distinguishing intrinsic narrow line systems (Barlow 1995; Hamann et al. 1996.) In the case of some narrow lines with $z_a \sim z_e$ the lines appear to be smoother with less component structure than most intervening systems; they also exhibit an effect which implies that the absorption-line region does not fully occult the background light source. This effect is inferred from the profiles of resolved lines in doublets such as C IV and N V. Motivated by these considerations we investigate here the nature of the associated lines in the radio-loud quasar PKS 0123+257.

2. Observations

The HIRES spectra for PKS 0123+257 were obtained during service observing with the Keck I telescope on September 11 and 12, 1995. We acquired 4 exposures of 40 minutes (in cloudy skies and a full moon). Three exposures were obtained with one echelle grating angle and one exposure with a different echelle angle in order to get complete wavelength coverage of the region 3700 to 6100 Å.

The spectra were detected as 38 echelle orders on a 2048^2 Tectronics CCD. Each exposure used a 0.86 arc-second slit (3 pixels) for a resolution of approximately 6.3 km s^{-1}. The actual resolution varies from about 6.0 to 6.5 km s^{-1} FWHM due to the change in dispersion across each echelle order. The signal-to-noise ratio (S/N) per 3 pixel resolution element ranged from 9 at 3900 Å to 26 at 5400 Å. The S/N also varies with the distance from the blaze on each order and the overlap between two setting angles. In particular, the setting with a single exposure had significantly lower S/N which creates low S/N regions in the red portion of the spectrum.

The data were reduced using our own reduction package which automatically traces the orders, removes cosmic ray events, and uses an optimal weighting scheme similar to that of Horne 1986 for extracting the spectra (cf. Barlow 1996, in preparation.) The wavelength calibration used low-order polynomial fits to a ThAr arc lamp exposure in each order, loosely constrained by the fits in adjacent orders. The calibration error is about 0.1 pixel (0.2 km s^{-1}) root-mean-square with up to a maximum error of about 0.3 pixels (0.6 km s^{-1}.) This is the relative error across the spectrum. The absolute wavelength error is about 0.3 pixels (0.6 km s^{-1}), estimated from the night sky emission lines. Altogether there can be up to $\sim$1 km s^{-1} error in the absolute wavelength value at any given pixel. The wavelengths are shifted to a vacuum, heliocentric scale.

Due to imperfect corrections for variations in the pixel-to-pixel response (flat field division), we estimate a error in the relative level of the spectrum of about 0.5% which appears to cause "undulations" on the scale of several pixels. This is estimated from spectra of bright stars taken previously with HIRES. In addition, there are fluctuations due to our technique of forcing adjacent echelle orders to match over common wavelengths. It is estimated that systematic flux errors of $\sim$10% may be present over $\sim$1000 km s^{-1} regions where the orders have overlapped in wavelength.

Figure 1 shows the HIRES data for PKS 0123+257 from the Lyα (H I λ1215) broad emission-line (BEL) to the C IV λ1549 BEL. The data were not flux calibrated and the spectrum has been continuum normalized. Note the low S/N regions in the red portion of the spectrum. Despite the artificial fluctuations left over from the order-splicing procedure, the relative strengths of the Lyα, N V λ1240, and C IV λ1549 BELs are evident. The $z_a \gtrsim z_e$ absorption can be seen just redward of the most prominent emission peaks. An emission line redshift of $z_e = 2.364$ is estimated by averaging the values measured from the Lyα and C IV emission peaks.

3. Analysis

3.1. Incomplete Occultation

In figure 2, we compare the various lines in the associated system on a velocity scale in which zero velocity is defined at z_e =2.364. There are three main absorption lines with the strongest absorption appearing at z_a=2.3693 or about 480 km s^{-1} redward of z_e. Note that the strongest Lyα absorption line appears to have a flat-bottomed structure suggesting that the line is saturated, yet it does not reach zero intensity. This is a indication that the absorbing gas clouds do not completely cover the background light source along our line-of-sight.

The velocity shift of 600 km/s redward of the Lyα and C IV emission peaks does not necessarily imply infall toward the QSO. It has been shown that the C IV and Lyα BEL peaks are systematically blue-shifted relative to the true redshift of the QSO (as determined by narrow forbidden lines) by 500 $\pm$200 km s^{-1} (Tytler and Fan 1992.) This implies that all

the absorption shown in figure 2 may be produced by material ejected outward from the central QSO engine. From other studies of line profile and velocity shift correlations, we know that C IV can be shifted by as much as 1000 km s^{-1} or more. However, the width of 3500 km s^{-1} for the C IV BEL in PKS 0123+257 suggests that the shift is closer to a few hundred km s^{-1} (cf. Brotherton et al. 1994a.) This suggests that the strongest absorption line may be close to zero outflow velocity with respect to the QSO.

If the absorbing gas temperature is ∼10,000 K, then the thermal widths for Lyα and C IV are about 21 and 6 km s^{-1}, respectively. Thus, the main C IV feature contains many thermal widths and is essentially resolved in our spectra. The main line is not smooth like conventional broad absorption-lines and shows some indication for narrow components. However, these components are not as distinct and well separated as the components which are often seen in intervening absorption complexes. Overlapping components and apparently large line widths (∼50 km s^{-1}) may be indicative of intrinsic rather than intervening absorption (Barlow 1995.)

The apparent partial coverage of the background light source can be investigated using two or more resolved lines from the same ion. The optical depth ratios should be equal to the ratios of the oscillator strengths of the lines (assuming $\lambda_1 \simeq \lambda_2$) if the absorption clouds cover the light source. If we have resolved the C IV lines we can calculate the optical depth by taking the natural logarithm of the residual intensity ($R.I.$) with the continuum and emission-line flux normalized to unity, $\tau = -\ln(R.I.)$. We demonstrate that this is *not* the case in the PKS 0123+257 system. We have scaled the optical depth of the C IV λ1550 line by a factor of two after measuring the residual intensity assuming complete coverage by the absorbing clouds. In figure 3, we have plotted the scaled λ1550 line (thick line) over the unscaled λ1548 line. This figure shows that the 1548 line does not go deep enough to match the strength predicted by increasing the optical depth of the red line by two. Therefore, both the main absorption system (at 480 km s^{-1}) and the bluer system (at 190 km s^{-1}) exhibit partial coverage. The error in the spectrum at the position of the C IV λ1548 line at 330 km s^{-1} is much larger than for the adjacent lines (these wavelengths fell within the inter-order gap of the best exposures). Given the depth of the red component, the data is consistent with a coverage fraction (see below) between 0.4 and 1.0.

Figure 4 shows the same analysis for N V. Although the data at these wavelengths have somewhat lower S/N, the lines appear to be consistent with complete coverage of the background light source. As a check of this analysis technique, we do the same comparison for the C IV lines in an absorption system at z_a=2.301 which is assumed to be due to an intervening absorber. As shown in figure 5, this absorption system is consistent with complete coverage.

3.2. Defining Fractional Coverage

We can also calculate the coverage fraction (C_f) from the measured residual intensities at the lowest points in the lines. C_f is defined as the fraction of the background light source, in this case the QSO continuum source or the emission-line region, apparently covered by the absorbing clouds (as defined by the formulas given below.) Therefore, the amount of light (on a normalized scale) apparently leaking through the absorption-line region (ALR) would be $1 - C_f$. If the coverage fraction at wavelength λ is $C_f(\lambda)$, then the *true* optical depth of a line at λ with the observed residual intensity $R(\lambda)$ is given by:

$$\tau(\lambda) = -\ln\left(\frac{R(\lambda) - 1 + C_f(\lambda)}{C_f(\lambda)}\right).$$

We neglect any smoothing of the line caused by the finite resolution of the spectrograph. An *apparent* column density per unit velocity can be derived as described in Savage and Sembach (1991): $N(v) \propto \tau / f\lambda$. It is assumed that $f_{blue}/f_{red} = 2$ and $\lambda_{blue} \simeq \lambda_{red}$. Let R_b be the residual intensity of the blue (stronger) line of the doublet and R_r be the residual intensity of the red line. We assume that C_f is the same for both lines. Equating the column densities derived from each line, $N_{blue}(v) = N_{red}(v)$, we have:

$$-\ln\left(\frac{R_b - 1 + C_f}{C_f}\right) = -2\ln\left(\frac{R_r - 1 + C_f}{C_f}\right),$$

$$C_f = \frac{1 + {R_r}^2 - 2R_r}{1 + R_b - 2R_r}.$$

If $R_r \leq R_b$, we assume $C_f = 1 - R_r$ and if $R_b < R_r^2$, we assume C_f=1.

The measured values of C_f for C IV are $0.94^{0.95}_{0.93}$ (1σ error limits) at 480 km s^{-1} and $0.63^{0.65}_{0.62}$ at 190 km s^{-1}. In figure 3, we have marked (3σ error limits) the value of $1 - C_f$. In the case of the line at 480

km s^{-1}, the fact that the mark is close to the bottom of the line indicates that the lines have high optical depth (*i.e.* are nearly saturated.) The width of the mark indicates the portion of the spectrum where the residual intensity was measured. The line at 190 km s^{-1} also appears to be nearly saturated even though the lowest part of the line only reaches a residual intensity of about 0.3.

The measured values of C_f for N V are $0.98\,^{1.00}_{0.96}$ (1σ error limits) at 480 km s^{-1} and $0.79\,^{1.00}_{0.62}$ at 190 km s^{-1}. In figure 4, we show the values for the N V lines. Here the 1σ error limits in the $1-C_f$ value are shown. Both systems appear to be consistent with complete coverage. Although the S/N is much lower near the N V lines, the measured value of $1-C_f$ is significantly lower ($\sim 2\sigma$) than $1-C_f$ for C IV for the strongest absorption line at 480 km s^{-1}. The value of C_f measured for the C IV line at 480 km s^{-1} is 0.94 (using the data between 472 and 492 km s^{-1}.) For the bluer line at 190 km s^{-1} (calculated between 182 and 196 km s^{-1}), C_f is about 0.63. Both of these values are significantly less than one ($> 3\sigma$.) For N V C_f is measured to be 0.98, and is consistent (within 1σ) with complete coverage.

For Lyα we do not have another Lyman line for comparison. However, the flatness of the bottom of the line at 480 km s^{-1} suggests that it is saturated. Using the bottom of the line as an estimate of the fractional coverage we get C_f=0.91. (This is only a lower limit if the line is not saturated.) This value is slightly less than for C IV. For Si IV C_f is $0.93\,^{1.00}_{0.88}$ (with 1σ errors). The noise near this line and the fact that the Silicon lines may not be as well resolved as the Carbon lines (assuming that a significant portion of the width is due to thermal broadening, rather than just cloud turbulence) makes this C_f value rather uncertain.

In table 1, we show our measured values for the residual intensities at the lowest point in the lines and our estimates for the coverage fractions. We also calculate column densities assuming C_f=1. Since we know that the coverage may be incomplete for all these lines, these values are actually lower limits. In column 7, we present conservative lower limit estimates using the values of C_f. The fact that the C IV blue line yields a lower value than the red line indicates that the lines are saturated. In this case, we would need to fit the lines with Voigt profiles to get accurate estimates of the column densities. Unfortunately, it is difficult to determine the component positions and FWHM values for such a complex system with several overlapping components. However, we do know that log(N(H I))$\lesssim$18.5 because a higher column density would show damping wings which are inconsistent with the data.

We make the hypothesis here that the filling-in or partial coverage of the lines is due to light from the broad emission-line region (BELR) leaking through (or around) the ALR. From the depths of the lines it is clear that at least some of the BELR is occulted by the absorbing clouds (i.e. the residual intensity at the bottom of the absorption lines is much less than the strength of the BELs.) In this scenario it is reasonable to assume that all of the continuum source is covered since the continuum producing region is generally thought to be much smaller than the BELR (by a factor on the order of 100, cf. Osterbrock 1993.) However it is expected that this simple assumption will not be strictly valid, since multiple regions of varying dimensions may contribute to the BEL and the continuum emitting regions (cf. Wills et al. 1993.) This hypothesis can be tested in that C_f we calculate should be related to the strength of the BEL at the position of the absorption line. This is qualitatively consistent with the fact that C_f is nearly unity for N V (weak BEL), larger for C IV (strong BEL), and larger still for Lyα which shows the highest emission line peak.

3.3. Incomplete Coverage of the Broad Emission-Line Region

Let us assume a relatively simple model where the amount of light at the wavelength of the absorption line which is leaking through or around the ALR is proportional to the strength of the BEL at that wavelength. At the position of the C IV absorption, the BEL level is 2.0 in continuum normalized units and C_f is 0.94 (where the BEL plus continuum has been normalized to one.) This means that $((1-0.94)\times 2.0)/(2.0-1) = 0.12$ of the BEL light is not occulted by the absorption clouds. For N V the BEL level is 1.3. This means that we would expect $C_f = 1-((0.3\times 0.12)/1.3) = 0.97$, which is consistent with our results. For Lyα the BEL is 2.9 from which we expect a $C_f = 1-((1.9\times 0.12)/2.9) = 0.92$, consistent with our estimated value of 0.91. However, this simple model does not apply to all the $z_a \sim z_e$ absorption lines. If we consider the line at 190 km s^{-1} redward of the emission redshift (see figure 3), we find that the C IV line has C_f=0.63.

This means that $(1-0.63)\times 2.0)/(2.0-1) = 0.74$ of the BEL light leaks through (assuming it covers the continuum completely). The N V line is too uncertain for comparison, but it is evident that the Lyα is much deeper than predicted. The predicted value is $C_f = 1-((1.9\times 0.74)/2.9) = 0.48$, but the actual C_f for Lyα must be at least 0.85 (see figure 2.)

We note here a few factors which may cause deviations from the simplest interpretation. (1) The position of the absorption lines over the BEL will effect our calculations. For example, since the emission is greater at the position of λ1548 than λ1550, this means that C_f values may be slightly over-estimated. In the case of Si IV the opposite is true, since the emission is weaker at the position of the blue line of the doublet. This is presumably due to the O IV] 1402 BEL and means that C_f may be slightly larger than calculated. And, in the case of N V , we have a BEL contribution from the red wing of Lyα. (2) A complex geometry for the BELR would imply that the size of the BELR (and hence the ability for the ALR to cover it) may vary with velocity and ion. In particular, there may be a narrow and broad component to the C IV BEL such that the broad component is blue shifted and arises in an emitting region closer to the QSO central engine than the narrow component (Brotherton et al. 1994b.) (3) The "effective" size of the ALR may vary with ionization level and/or optical depth. For example, the geometry of the portion of the region with relatively high amounts of Si IV may be different than the geometry of the portion of the ALR with relatively high amounts of C IV. In another study of narrow intrinsic lines in the QSO UM 675 (Hamann et al. 1996), it is noted that C_f for C IV must be substantially less than that for Lyα.

We can reconcile the earlier results by appealing to factor (3). We hypothesize that the ALR has a fixed boundary which is smaller than the apparent size of the BELR as seen along our line-of-sight. This means that there is a maximum line depth which occurs when the optical depth is very high and the clouds occult all lines-of-sight through the ALR. This is the case for the strongest absorption lines in PKS 0123+257, *e.g.* C IV, N V, and Lyα. However, if the column density of absorbing gas varies between different lines-of-sight through the ALR, then at lower optical depth we get an *effective* C_f which is significantly smaller. This is because the various lines-of-sight will contribute much differently to the line profile. In this scenario, we imagine that the observed absorption line is composed of a superposition of profiles from clouds with a range of column densities and a range of C_f. For example, we suppose that there exists two sub-regions in the ALR which cover different lines-of-sight. If we could look only through sub-region #1 we would measure an optical depth of $\tau \sim 2$, and if we looked only through sub-region #2 we would measure $\tau \sim 0.1$. In practice, we observe the sum of the light going through both sub-regions. If the first sub-region covers only 50% of the source then would measure $C_f \sim 0.5$, since the second sub-region contributes little to the observed line profile. Let us now increase the optical depth of both regions by a factor of 5. Since the optical depth in sub-region #1 was already fairly high, these clouds contribute only a little more to the depth of the line, but the clouds of the sub-region #2 now contribute much more. The line becomes deeper and C_f increases. This means that the *effective* C_f can vary depending on the optical depth of a given transition without changing the geometry of the clouds or the region. In this scenario, factor (3) can cause a variation in the effective C_f for different ions *and* for different lines of the same ion. Note that this complicates what we mean by partial coverage. In this model, we cannot define partial coverage as simply the fraction of sight lines which pass through absorbing gas.

Applying these ideas to our results, the system at 190 km s^{-1} (see figure 2) has clouds which can cover at least 85% of the background light source as shown by the Lyα line. However, the lines-of-sight through this region have varying column density such that the less abundant C^{+3} ions only contribute significantly to the line strength in certain sub-regions. These sub-regions are only able to effectively cover about 63% of the background light source. Note that in this model we do *not* need to vary the ionization level among the clouds in the ALR, we only need to vary the column density looking through different lines-of-sight toward the light source.

We can also use this model to explain the Si IV in the main system at 480 km s^{-1}. Above we measured C_f of Si IV to be 0.93 with a large error. This value appears to be larger than the value for N V even though the N V BEL is stronger than the Si IV BEL. This is inconsistent with the simple analysis we discussed at the beginning of this subsection for this absorption system. The explanation here is that the line is weak and thus we must appeal to factor (3), *i.e.* the Si^{+3} ions in the lower column density lines-of-

sight to not contribute substantially to the line depth, and therefore for Si IV we do not get a C_f which is proportional to the BEL strength.

4. Discussion

4.1. Difficulty of Determining Column Densities

Once we have absorbing clouds which do not cover the background light source a range of effects must be considered when interpreting the depth and profile of a line for the purpose of deriving column densities. When all the effects discussed above are considered, we can appreciate the difficulty in determining accurate column densities. If we were to calculate the column densities assuming complete coverage in this object, we would get values for C IV, N V and Lyα from which we could estimate ionization levels and abundances. In reality these values are inaccurate since the lines are actually nearly saturated and the varying depths are not caused simply by differences in ionic abundance, but rather they are determined largely by differences in the fractional coverage of the BELR.

Recently there has been work done on the metallicity and ionization levels in intrinsic absorption systems. In 0226-1024, Korista et al. (1996) use ground-based and HST spectra of numerous transitions to deduce enhanced metal abundances for the absorbing gas relative to solar. In UM 675, Hamann et al. (1995) argue for stratified regions of greatly differing ionization levels. In PG 0946+301, Junkkarinen et al. (1995) argue for Phosphorus abundances two orders of magnitude greater than solar. And using high resolution spectroscopy of two QSOs, Petitjean et al. (1994) argue for increased metallicities for absorption systems near the emission-line redshift. The success of line fitting and ionization estimates for these systems indicates that these results are, in general, accurate. However, all of these results should be considered in the context of the problems with studying intrinsic absorption lines as discussed above. The possibility of partial coverage has been discussed in some of these works, but not yet applied.

4.2. Determining the Causes of Partial Covering

We discussed above the nature of the coverage fraction varying among the lines. This effect can result from a number of causes. If, for example, we were to see a different C_f for Si IV and C IV, we could explain this result if the ionization or the optical depth varies between different lines-of-sight through the ALR. It will be possible to test which of these effects is dominant by studying C_f deduced from lines of different ions and different lines due to the same ion. We note that if this model is valid, then even the two members of the C IV doublet will have different C_f, making the determination of C_f and the column densities even more problematic. Furthermore, one would expect C_f to also change in a time variable system if the variability is due to a change in ionization level, *i.e.* as the fractional abundance of an ion varies so does the optical depth in the line. This effect can be tested using high resolution spectra of a time variable absorption system (as seen in the QSO 2343+1232, Hamann et al. 1996b.)

4.3. Failure to Distinguish Intrinsic Systems

None of the seven methods mentioned in the introduction are conclusive tests for intrinsic vs. intervening systems. For example, in the QSO 2116-358, Wampler et al. 1993 show a system which suggests partial coverage of the BEL in the Si III λ1206 line; yet the same system does not show absorption from excited fine structure lines and thus must be a large distance (>1 kpc) from the QSO nucleus. It will be necessarily to investigate these seven qualities statistically in many objects to determine how best to discriminate intrinsic absorbers.

4.4. Radio-Loud Quasars

An excess of $z_a \sim z_e$ systems in radio-loud quasars relative to radio-quiet quasars has been noted by previous studies (cf. Anderson et al. 1987). In this paper, we have shown that a $z_a \sim z_e$ system in a radio-loud quasar shows a property (namely $C_f < 1$) in common with other intrinsic systems seen in radio-quiet quasars. While there is an excess of $z_a \sim z_e$ systems in radio-loud quasars, there is a definite lack of $z_a \ll z_e$ systems (*i.e.* BALs.)

Recent work on high redshift radio galaxies has shown a frequent occurrence $z_a \sim z_e$ Lyman-α absorption (van Ojik et al. 1996). The large fraction of galaxies with such absorption (60%) implies that the absorbing gas is intrinsic to the host galaxy. Long-slit spectra show that the absorbing region extends over the entire emitting region (up to ∼50 kpc.) Also, a correlation is found between the size of the radio jet

and the Lyman-α emitting region. What is the connection between the radio jet and the gas giving rise to associated absorption? Why is there a lack of accelerated ($z_a \ll z_e$) intrinsic systems in radio bright sources? How are the emitting and absorbing regions related in quasars? We may be able to answer these questions by identifying and studying intrinsic systems in both radio-loud and radio-quiet objects.

5. Summary

In this paper we have presented high resolution spectroscopy of the $z_a \sim z_e$ intrinsic absorption system in the radio quasar PKS 0123+057. The data are consistent with the conclusion that the background light source (which in this case includes both the continuum and broad emission-line region) is not fully occulted by the gaseous region causing this absorption. This is deduced both from the profile of the Ly-α absorption line and the residual intensities of the C IV doublet. The derived coverage fractions, C_f, of the strongest absorption lines are inversely proportional with the strength of the corresponding emission-lines, which indicates that the absorption-line region obscures no more than about 88% of the light from the emission-line region. Furthermore, the coverage fractions measured for the weaker lines are consistent with a model where the absorption-line region is inhomogeneous through the various lines-of-sight towards the emission-line region which pass through the absorbing gas. This model shows that, for weak lines, the calculated value of C_f decreases with the depth of the absorption line. These effects mean that the optical depths measured using the assumption that the absorbing gas homogeneously and completely covers the background light source would significantly underestimate the true column density through the absorption-line region. Furthermore, the degree to which the column densities are underestimated will vary with the strength of the absorption line. Accurate analyses of metal abundances in the gaseous environment near QSOs using intrinsic absorption systems must necessarily account for these factors.

We thank T. Bida and R. Campbell of Keck Observatory for obtaining these data via service observing. We are grateful to F. Hamann, V. Junkkarinen, and R. Cohen for useful discussions. We also thank N. Arav and D. Hogg for discussions regarding partial coverage of intrinsic absorption lines. This work was supported by grants AST92-21365 and AST95-29073 from the National Science Foundation.

REFERENCES

Anderson, S. F., Weymann, R. J., Foltz, C. B., and Chaffee, F. H., Jr. 1987, AJ, 94, 278

Bahcall, J. N. 1968, ApJ, 153, 679

Barlow, T. A., Junkkarinen, V. T., Burbidge, E. M., Weymann, R. J., Morris, S. L., and Korista, K. T. 1992, ApJ, 397, 81

Barlow, T. A. 1993, Ph.D. thesis, Univ. of California, San Diego

Barlow, T. A. 1995, BAAS, 27, 872

Barthel, P.D. 1988, in ESO Mini-Workshop on Quasar Absorption Lines, ed. P.A. Shaver, E.J. Wampler, and A.M. Wolfe (Garching: ESO), 79

Briggs, F. H., Turnshek, D. A., and Wolfe, A. M. 1984, ApJ, 287, 549

Brotherton, M. S., Wills, B. J., Steidel, C. C., and Sargent, W.L.W. 1994a, ApJ, 423, 131

Brotherton, M. S., Wills, B. J., Francis, P. J., and Steidel, C. C. 1994b, ApJ, 430, 495

Carswell, R. F., Coleman, G., Strittmatter, P. A., and Williams, R. E. 1976, A&A, 53, 275

Cohen, M. H., Ogle, P. M., Tran, H. D., Vermeulen, R. C., Miller, J. S., Goodrich, R. W., and Martel, A. R. 1995, ApJ, 448, L77

Foltz, C. B., Weymann, R. J., Peterson, B. M., Sun, L., Malkan, M. A., and Chaffee, F. H., Jr. 1986, ApJ, 307, 504

Foltz, C. B., Chaffee, F. H., Jr., Weymann, R. J., and Anderson, S. F. 1988, in *QSO Absorption Lines: Probing the Universe,* eds. J. C. Blades, D. A. Turnshek, and C. A. Norman (Cambridge: Cambridge Univ. Press), p. 53

Goodrich, R. W., and Miller, J. S. 1995, ApJ, 448, L73

Hamann, F., Barlow, T. A., Beaver, E. A., Burbidge, E. M., Cohen, R. D., Junkkarinen, V., and Lyons, R. 1995, ApJ, 443, 606

Hamann, F. 1996, submitted to ApJS

Hamann, F., Barlow, T. A., Beaver, E. A., Burbidge, E. M., Cohen, R. D., Junkkarinen, V., and Lyons, R. 1996, submitted to ApJ

Hamann, F., Barlow, T. A., and Junkkarinen, V. 1996, submitted to ApJ

Horne, K. 1986, PASP, 98, 609

Junkkarinen, V. T., Beaver, E. A., Burbidge, E. M., Cohen, R. D., Hamann, R. W., Lyons, R. W., and Barlow, T. A. 1995, BAAS, 27, 872

Korista, K. T., Hamann, F., Ferguson, J., and Ferland, G. 1996, ApJ, 461, 641

Morris, S. L., Weymann, R. J., Foltz, C. B., Turnshek, D. A., Shectman, S., Price, C., and Boroson, T. A., ApJ, 310, 40

van Ojik, R., Röttgering, H. J. A., Miley, G. K., and Hunstead, R. W. 1996, preprint.

Osterbrock, D. E. 1993, ApJ, 404, 551

Petitjean, P., Rauch, M., and Carswell, R. F. 1994, A&A, 291, 29

Sargent, W. L. W., Boksenberg, A., and Steidel, C. C. 1988, ApJS, 68, 539

Savage, B. D. and Sembach, K. R. 1991, ApJ, 379, 245

Schmidt, M., and Olsen, E. T. 1968, AJ, 73, S117

Tytler, D., and Fan, X. M. 1992, ApJS, 79, 1

Wampler, E. J., Bergeron, J., and Petitjean, P. 1993, A&A, 273, 15

Wampler, E. J., Chugai, N. N., and Petitjean, P. 1995, ApJ, 443, 586

Weymann, R. J., Williams, R. E., Peterson, B. M., and Turnshek, D. A. 1979, ApJ, 234, 33

Williams, R. E., Strittmatter, P. A., Carswell, R. F., and Craine, E. R. 1975, ApJ, 202, 296

Wills, B. J., Brotherton, M. S., Fang, D., Steidel, C. C., and Sargent, W. L. W. 1993, ApJ, 415, 563

This 2-column preprint was prepared with the AAS LaTeX macros v4.0.

Fig. 1.— HIRES spectrum of PKS 0123+257 with the prominent emission lines marked. The data has been binned such that each pixel is 21 km s^{-1} wide. The continuum (but not the emission-lines) has been normalized to one. The associated absorption lines can be seen just redward of the emission peaks.

Fig. 2.— The associated absorption system at z_a=2.369 shown on a velocity scale where zero velocity is at z_e=2.364. The continuum and emission line flux have been normalized to one. There are 3 pixels for each 6.3 km s^{-1} FWHM resolution element.

Fig. 3.— The C IV associated absorption complex. C IV λ1548 is shown as a thin line and C IV λ1550 as a thick line. The optical depth of the 1550 Å line has been scaled by a factor of two. Each bin is 4.2 km s^{-1} wide and the 1σ error per bin for the 1548 Å line is shown as a dotted line. Also marked are the estimated values of $1-C_f$ (with 3σ error bars) for the lines at 190 km s^{-1} and 480 km s^{-1} inflow relative to z_e.

Fig. 4.— The N V associated absorption complex. N V λ1238 is shown as a thin line and N V λ1242 as a thick line. The optical depth of the 1242 Å line has been scaled by a factor of two. Each bin is 4.2 km s^{-1} wide and the 1σ error per bin for the 1238 Å line is shown as a dotted line. Also marked are the estimated values of $1-C_f$ (with 1σ error bars) for the lines at 190 km s^{-1} and 480 km s^{-1}.

Fig. 5.— The C IV lines for a $z_a < z_e$ absorption system at z_a=2.301 plotted as in figure 3 with the 1550 Å optical depth increased by a factor of two. Zero velocity is set to z_a=2.301.

TABLE 1
ABSORPTION LINE MEASUREMENTS

Line	$\lambda_{\rm obs}$ (Å)	Velocity[a] (km s^{-1})	R[b]	C_f[c]	log(N) ($C_f = 1$)	log(N) ($C_f < 1$)
Lyα λ1215	4083.0	+480	0.092	>0.91	14.7	> 14.9
N V λ1238	4160.7	+480	0.033	$0.98\ ^{1.00}_{0.96}$	14.8	> 14.8
N V λ1242	4174.1	+480	0.146	···	14.8	> 14.8
Si IV λ1393	4681.1	+480	0.107	$0.93\ ^{1.00}_{0.88}$	13.6	> 13.7
Si IV λ1402	4711.4	+480	0.254	···	13.6	> 13.7
C IV λ1548	5199.8	+480	0.063	$0.94\ ^{0.98}_{0.91}$	14.6	> 14.8
C IV λ1550	5208.5	+480	0.082	···	14.8	> 15.0
Lyα λ1215	4086.9	+190	0.154	>0.85	14.0	> 14.1
N V λ1238	4164.8	+190	0.426	$0.79\ ^{1.00}_{0.62}$	13.7	> 13.8
N V λ1242	4178.2	+190	0.623	···	13.6	> 13.7
Si IV λ1393	4685.6	+190	···	···	···	···
Si IV λ1402	4715.9	+190	···	···	···	···
C IV λ1548	5204.9	+190	0.367	$0.63\ ^{0.70}_{0.59}$	13.6	> 14.0
C IV λ1550	5213.5	+190	0.372	···	13.8	> 14.2

[a]Relative to z_e=2.364.

[b]Residual intensity at lowest point of absorption line.

[c]Coverage fraction limits are 3σ for C IV, 1σ for N V and Si IV.

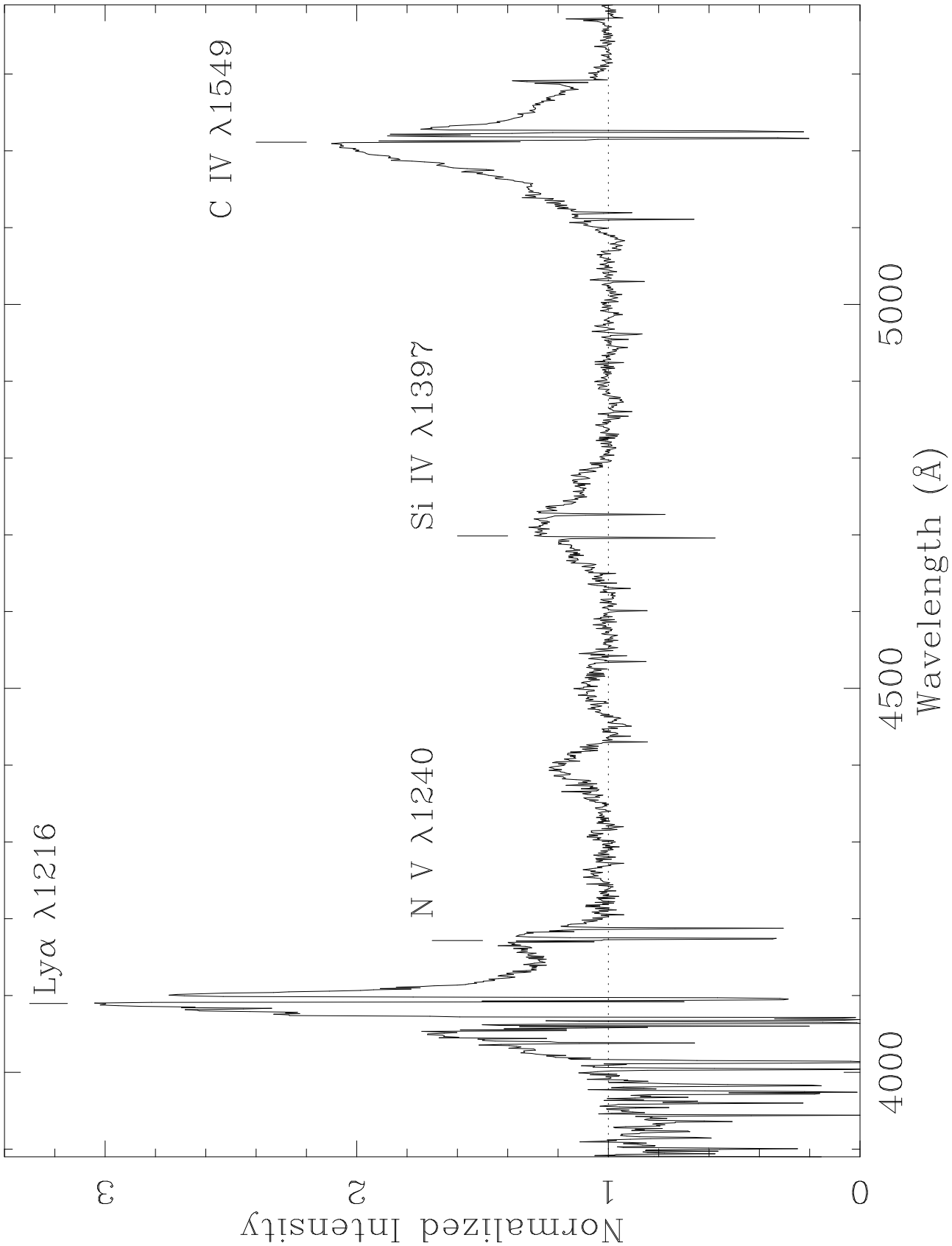

Fig. 1.— see figure caption page

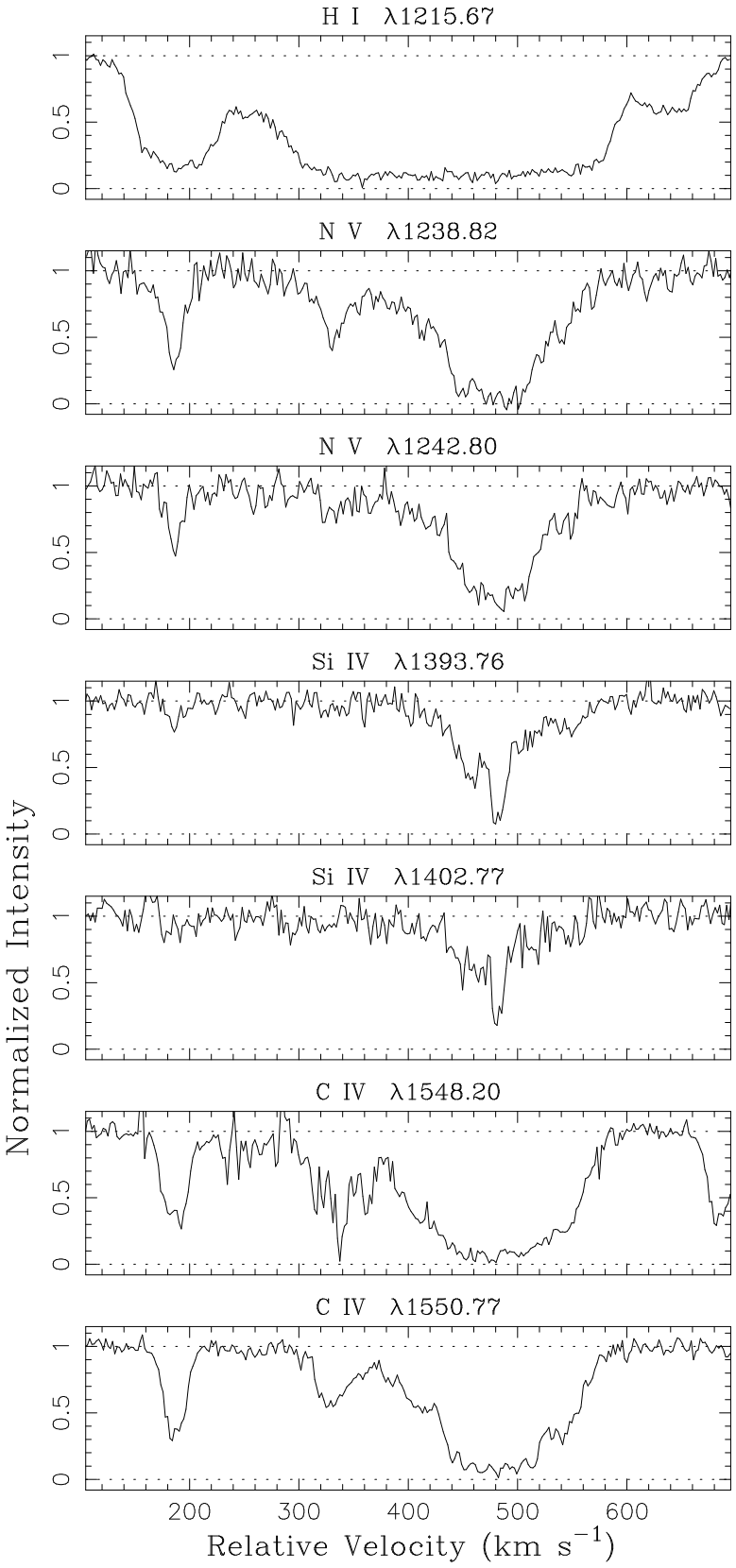

Fig. 2.— see figure caption page

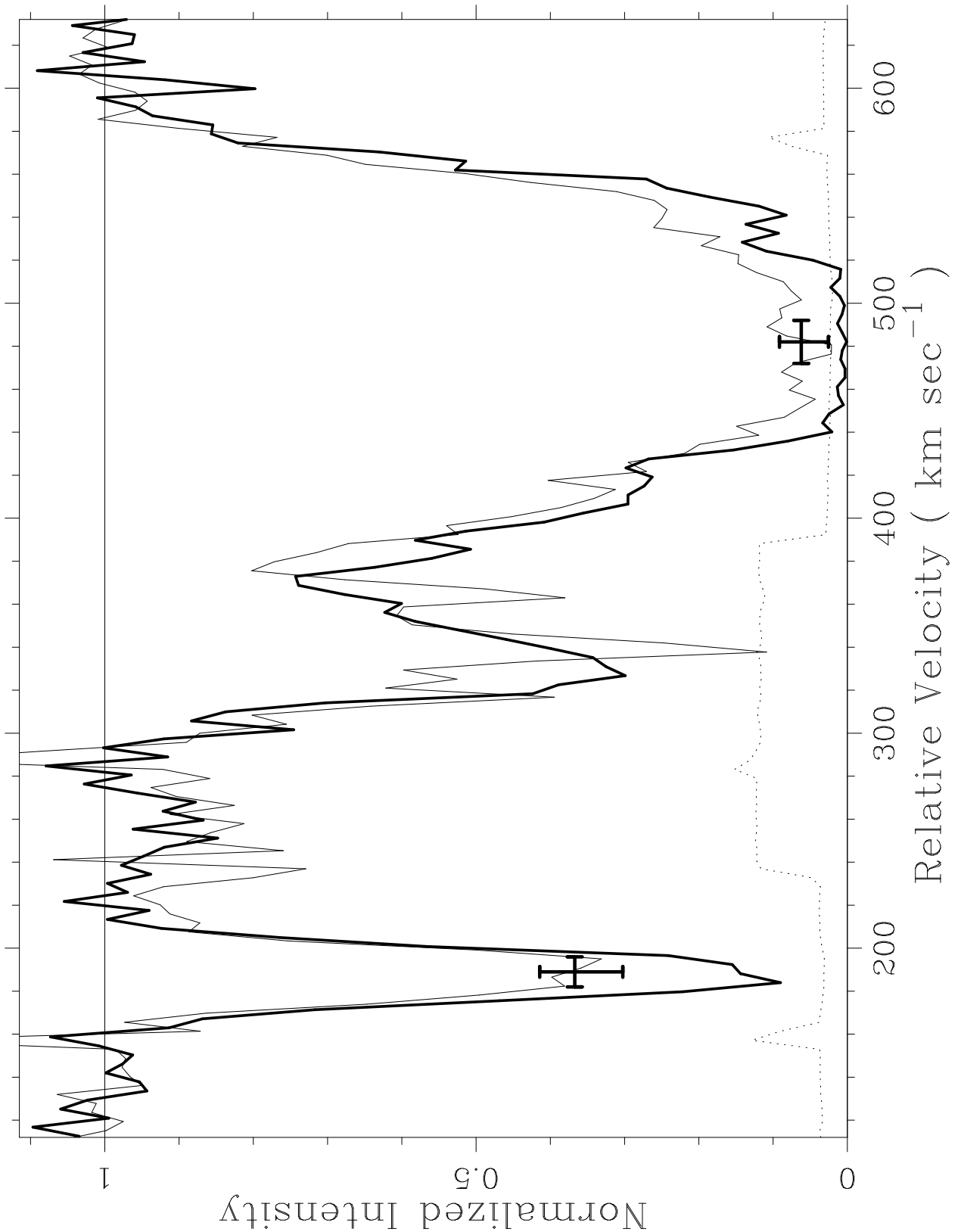

Fig. 3.— see figure caption page

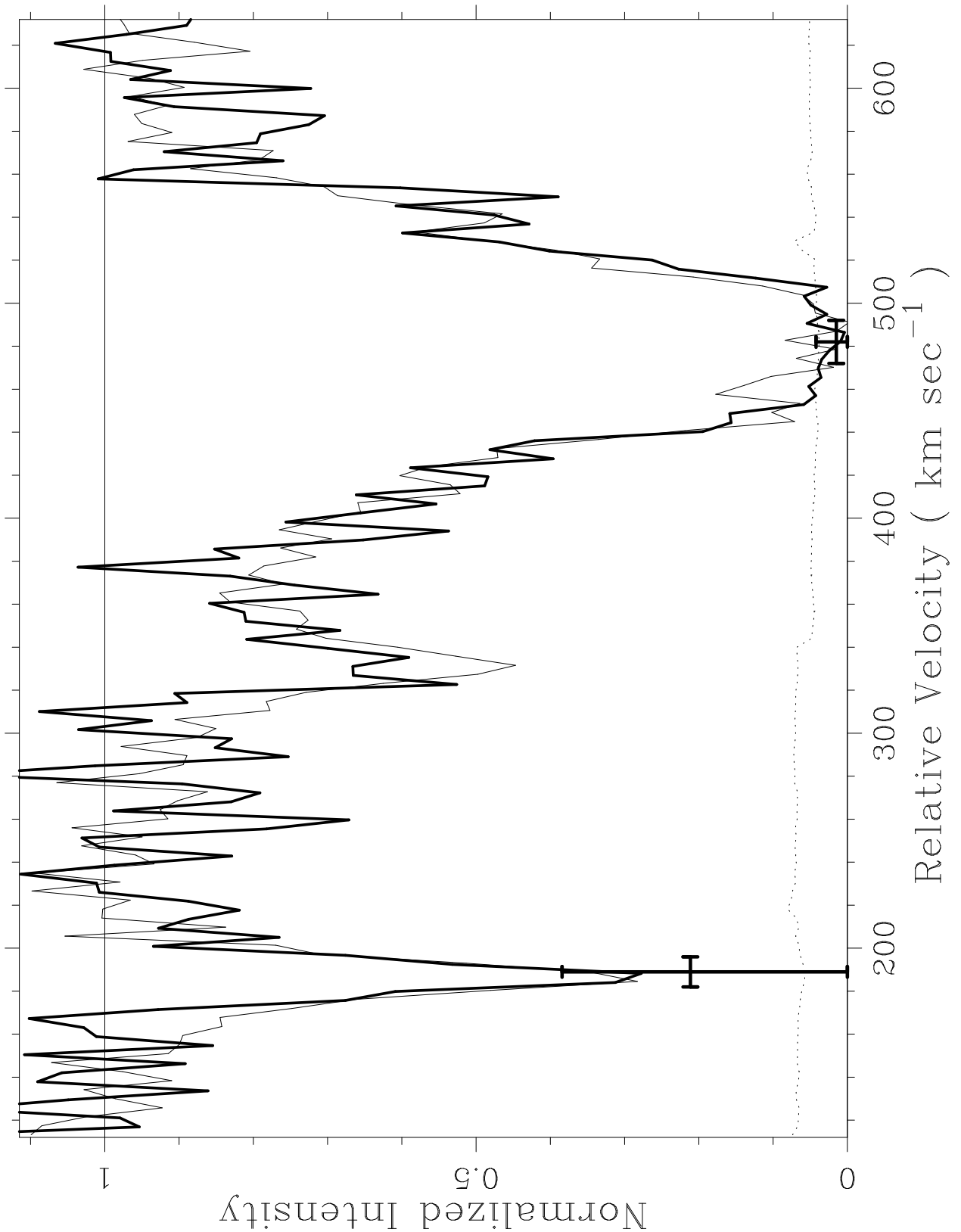

Fig. 4.— see figure caption page

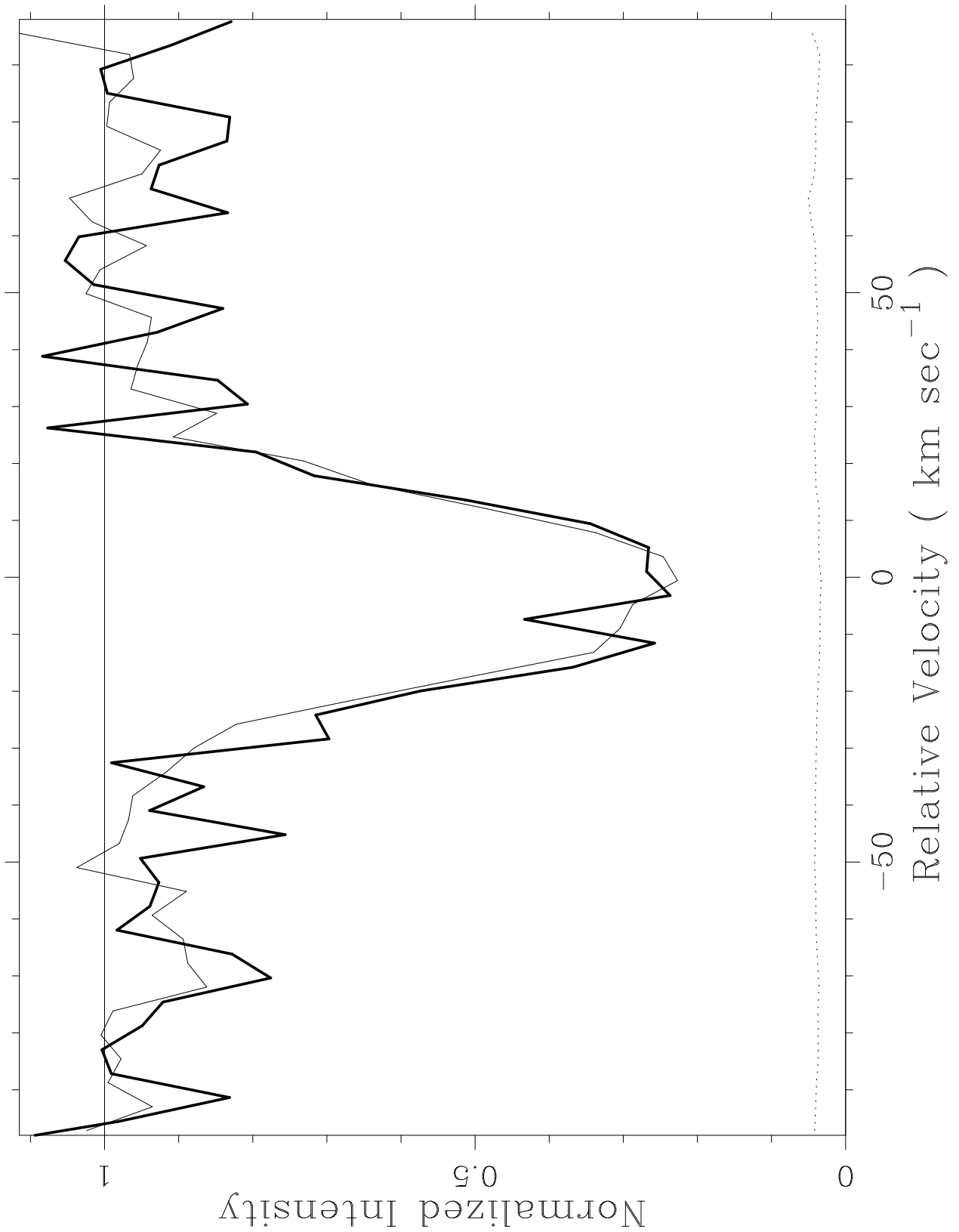

Fig. 5.— see figure caption page